Supporting Information for: Electropolymerization of Au nanoparticle incorporated poly(dopamine) thin-films at a micro liquid|liquid interface

Leila Nazari,[a] Fanqi Kong,[b] E. Bradley Easton,[b] and Talia Jane Stockmann[a,*]

[a] Department of Chemistry, Core Science Facility, Memorial University of Newfoundland, 45 Artic Ave, St. John's, NL, Canada, A1C 5S7. Email: tstockmann@mun.ca

[b] Ontario Tech University, 2000 Simcoe Street North, Oshawa, ON L1G 0C5, Canada

Table of Contents

1. Simple ion transfer voltammetry of $AuCl_4^-$ at increasing pH

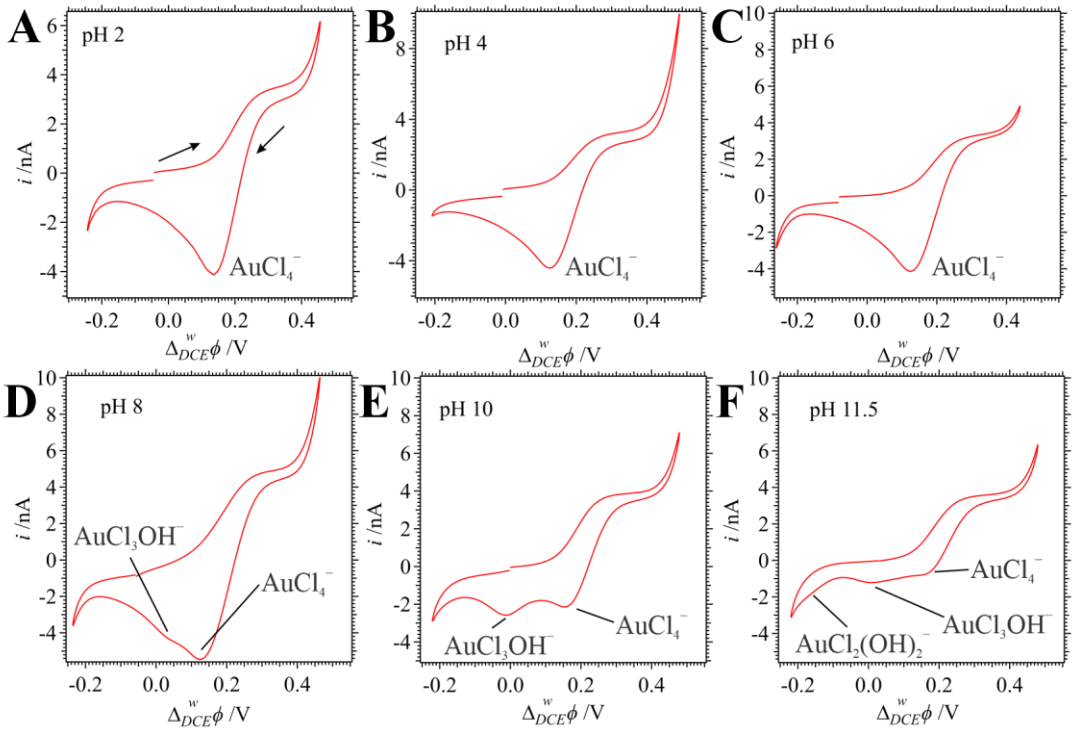

Figure S1: Cyclic voltammograms (CVs) recorded at 0.020 V s^{-1} using Cell 1 with 2 mM of $P_{66614}AuCl_4$ in DCE and no dopamine (DA) added to the aqueous phase, while increasing the pH from 2 to 11.5 (**A-F**) as indicated inset. The peaks have been labelled inset indicating the Au-ligand species undergoing ion transfer from w → DCE according to their order of appearance and the work of Luty-Błocho *et al.*;[1] however, this is speculative considering the lack of tandem spectroscopic analysis for confirmation.

2. Au nanoparticle/polydopamine nanocomposite characterization

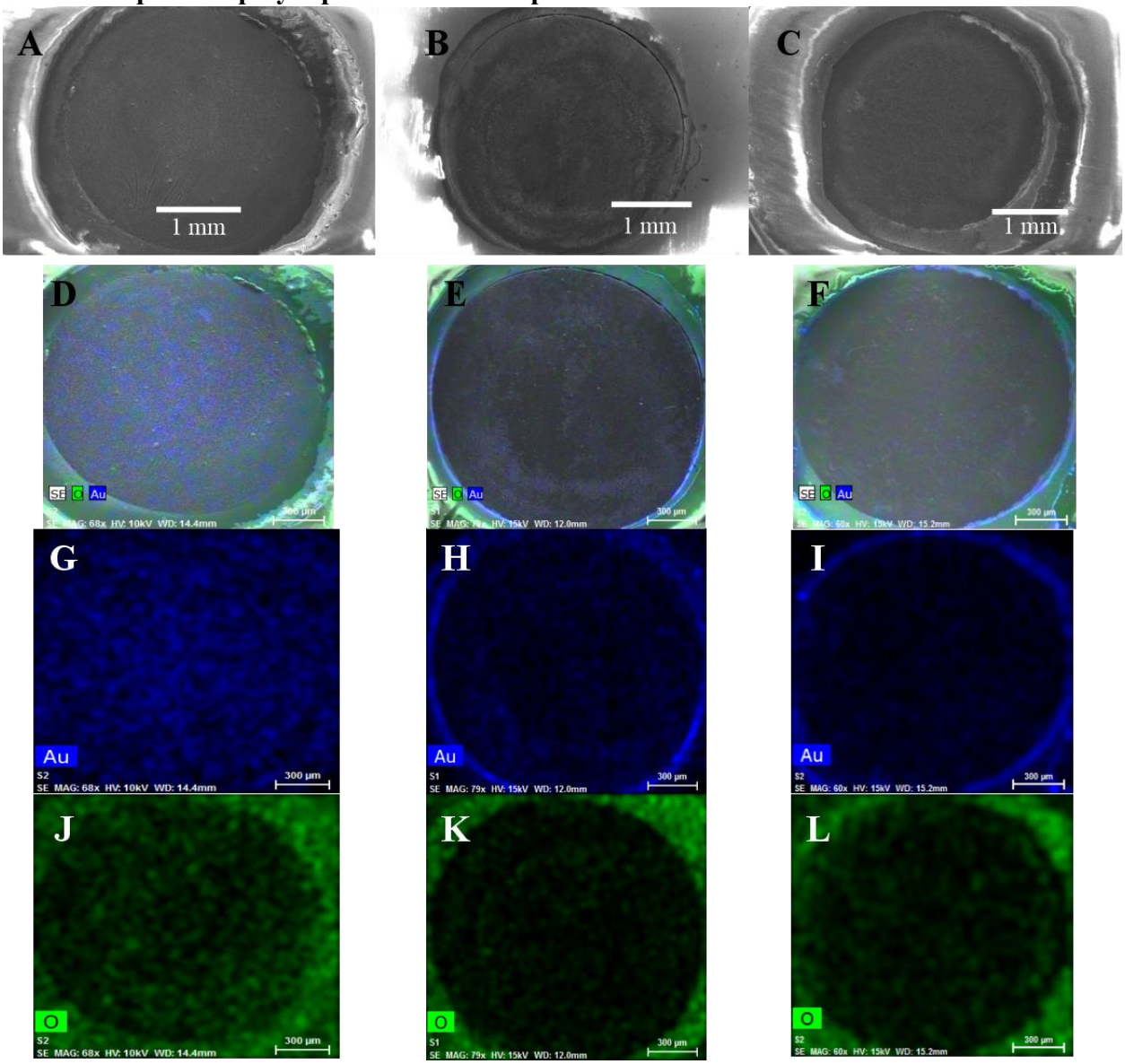

Figure S2: (**A-C**) Scanning electron microscopy images of Au NP/poly(DA) films deposited onto glassy-carbon electrodes (GCE). Films were generated using Cell 1 (see Scheme 1 of the main text) with $[DA]_{DCE}$ = 20 mM after 25 CV cycles at 0.020 V s^{-1}. The aqueous phase as adjusted to pH 4 (**A**, **D**, **G**, **J**), 8 (**B**, **E**, **H**, **K**), and 10 (**C**, **F**, **I**, **L**). At pH > 8, the aqueous solution was bubbled with N_2 gas (99.99%, Linde/Praxair) for ~20 min to displace and dissolved O_2. Panels **D-L** show EDX elemental maps of Au and O distribution on the surface.

3. Determination of $AuCl_4^-$ reduction potential and thermodynamic calculations

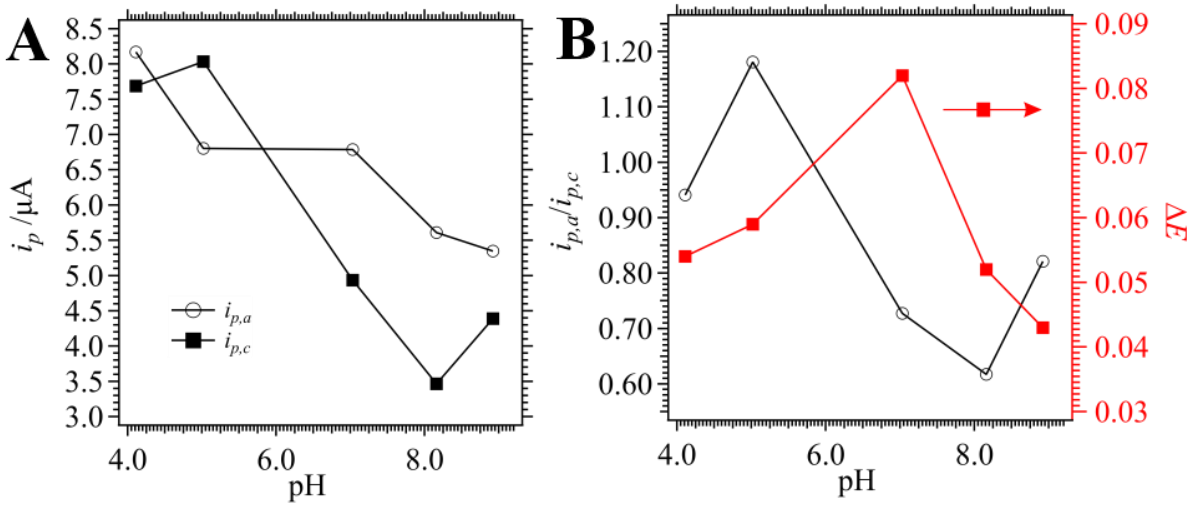

Figure S3: Plots of i_p (**A**), $i_{p,a}/i_{p,c}$, and ΔE (**B**) versus pH taken from voltammetric data presented in Figure 5B of the main text. Red arrow indicates the axis the curve is plotted against.

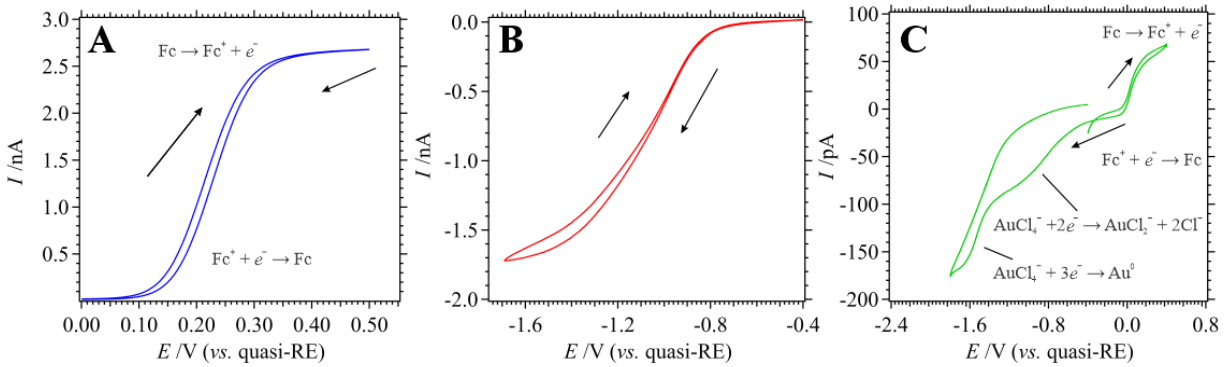

Figure S4: Cyclic voltammograms recorded using an inlaid disc carbon fiber ultramicroelectrode (UME), r = 3.5 µm, and an Ag wire as CE/quasi-RE at a scan rate of 0.020 V s^{-1} in DCE with 5 mM $P_{8888}TB$ as supporting electrolyte and either 1 mM Fc (**A**), 1 mM $P_{66614}AuCl_4$ (**B**), or both (**C**). The redox reactions are indicated inset in C, while the black arrows indicate scan direction.

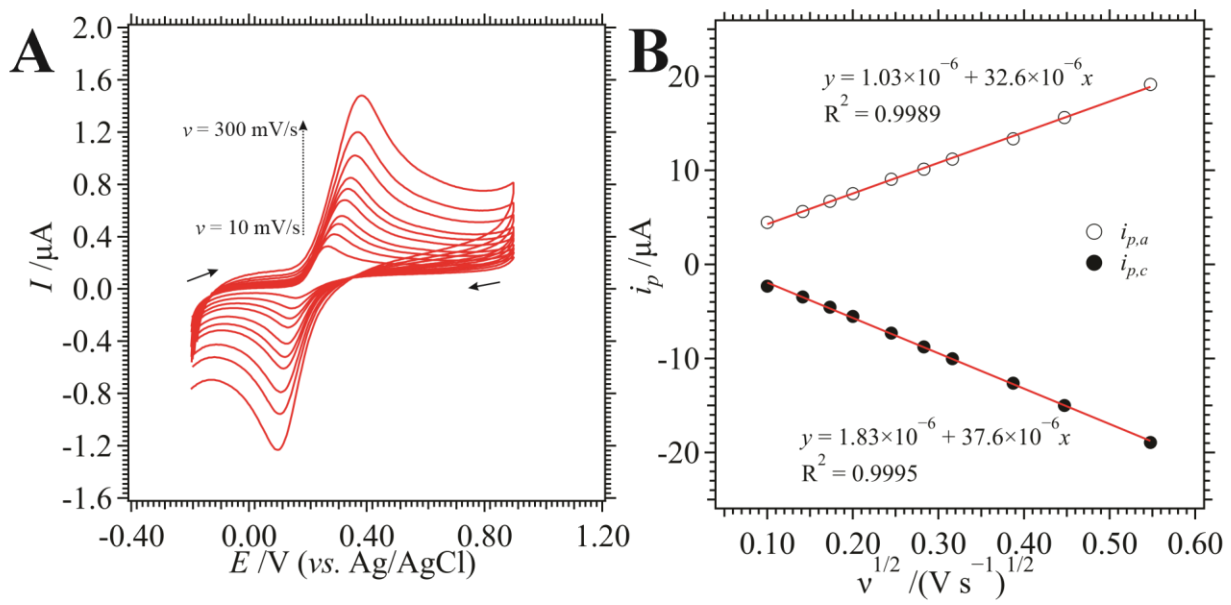

Figure S5: (**A**) Cyclic voltammograms (CVs) recorded at a glassy-carbon electrode (GCE) modified with a Au NP/PDA film electrogenerated using Cell 1 (see the main text) at pH 4, [DA] = 20 mM, and 25 CV cycles. CVs in A were recorded in a 3-electrode mode with 0.1 M KCl supporting electrolyte and 0.3 mM of DA added to the aqueous solution. The scan rate was increased as indicated inset. The black, solid arrows indicate scan direction. (**B**) Plots of the anodic ($i_{p,a}$, ○) and cathodic ($i_{p,c}$, ●) versus $\nu^{1/2}$. Solid lines were generated via linear regression and the correlation coefficients (R^2) and linear equations have been given inset.

4. Error associated with linear regression analysis

The upper and lower error bounds for the *line-of-best-fit* (LOBF) was determined using a method described in Skoog *et al.*[2] where the standard deviation (s_c) about the LOBF is defined as,

$$s_c = s_r \sqrt{\frac{1}{N} + \frac{N(x-\bar{x})^2}{N\sum x^2 - \left(\sum x\right)^2}}$$

where s_r is the standard error from linear regression statistics and the upper and lower error bounds are,

Upper LOBF+ = $y = mx + b + ts_c$

Lower LOBF– = $y = mx + b - ts_c$

In this case, t is students t-value taken from standard tables using a 99.9% confidence interval (t-value = 7.173) and *degrees-of-freedom* as defined as $N - 2$, where N is the population or number of data points used to construct the curve.

5. Theory

Interfacial Electron Transfer

From the general equation for the thermodynamics of interfacial electron transfer[3] and reaction [4] in Scheme 3 of the main text, one can obtain,

$$\Delta_o^w\phi_{\mathrm{ET}} = E^{o',\mathrm{H_2O}}_{DA^{2+}/\mathrm{DA}} - E^{o',\mathrm{DCE}}_{\mathrm{Au(III)}/\mathrm{Au}} + \frac{RT}{n_{\mathrm{DA^{2+}/Fc}}\, n_{\mathrm{Au(III)}/\mathrm{Au}}\, F}\ln\left(\frac{\left[\mathrm{Cl^-}\right]^4\left[\mathrm{H^+}\right]^6}{\left[\mathrm{AuCl_4}\right]^2\left[\mathrm{DA}\right]^3}\right)$$

$$\Delta_o^w\phi_{\mathrm{ET}} = E^{o',\mathrm{H_2O}}_{DA^{2+}/\mathrm{DA}} - E^{o',\mathrm{DCE}}_{\mathrm{Au(III)}/\mathrm{Au}} + \frac{RT}{6F}\left[\ln\left(\frac{\left[\mathrm{Cl^-}\right]^4}{\left[\mathrm{AuCl_4}\right]^2\left[\mathrm{DA}\right]^3}\right) + \ln\left[\mathrm{H^+}\right]^6\right] \qquad \text{[S1]}$$

$$\Delta_o^w\phi_{\mathrm{ET}} = E^{o',\mathrm{H_2O}}_{DA^{2+}/\mathrm{DA}} - E^{o',\mathrm{DCE}}_{\mathrm{Au(III)}/\mathrm{Au}} + \frac{RT}{6F}\ln\left(\frac{\left[\mathrm{Cl^-}\right]^4}{\left[\mathrm{AuCl_4}\right]^2\left[\mathrm{DA}\right]^3}\right) - \frac{RT}{F}\ln\left[\mathrm{H^+}\right]$$

For simplicity if one neglects the 3rd term on the right-hand side, then,

$$\Delta_o^w\phi_{\mathrm{ET}} \approx E^{o',\mathrm{H_2O}}_{DA^{2+}/\mathrm{DA}} - E^{o',\mathrm{DCE}}_{\mathrm{Au(III)}/\mathrm{Au}} + \frac{RT}{F}\ln\left[\mathrm{H^+}\right] \approx E^{o',\mathrm{H_2O}}_{DA^{2+}/\mathrm{DA}} - E^{o',\mathrm{DCE}}_{\mathrm{Au(III)}/\mathrm{Au}} - \frac{RT}{F}(\ln 10)\,\mathrm{pH} \qquad \text{[S2]}$$

For most cases $\gamma = 1$ and thus eq. S2 can be further reduced to,

$$\Delta_o^w\phi_{\mathrm{ET}} \approx E^{o',\mathrm{DCE}}_{\mathrm{Fc^+}/\mathrm{Fc}} - E^{o',\mathrm{H_2O}}_{\mathrm{Au(III)}/\mathrm{Au}} - (0.0257\ \mathrm{V})(\ln 10)\,\mathrm{pH} \qquad \text{[S3]}$$

Homogeneous Electron Transfer

For the homogeneous case of electron transfer, one begins with the more regular formulation of the Nernst equation,

$$E_{cell} = E^{o',\mathrm{H_2O}}_{\mathrm{Au(III)}/\mathrm{Au}} - E^{o',\mathrm{H_2O}}_{\mathrm{DA^{2+}}/\mathrm{DA}} - \frac{RT}{n_{\mathrm{DA^{2+}/Fc}}\, n_{\mathrm{Au(III)}/\mathrm{Au}}\, F}\ln\left(\frac{\left[\mathrm{Cl^-}\right]^4\left[\mathrm{H^+}\right]^6}{\left[\mathrm{AuCl_4}\right]^2\left[\mathrm{DA}\right]^3}\right)$$

$$E_{cell} = E^{o',\mathrm{H_2O}}_{\mathrm{Au(III)}/\mathrm{Au}} - E^{o',\mathrm{H_2O}}_{\mathrm{DA^{2+}}/\mathrm{DA}} - \frac{RT}{6F}\left[\ln\left(\frac{\left[\mathrm{Cl^-}\right]^{(4-\gamma)}\left[\mathrm{Fc^+}\right]^3}{\left[\mathrm{AuCl_{(4-\gamma)}(OH)_\gamma^-}\right]\left[\mathrm{Fc}\right]^3}\right) + \ln\left[\mathrm{H^+}\right]^6\right] \qquad \text{[S4]}$$

$$E_{cell} = E^{o',\mathrm{H_2O}}_{\mathrm{Au(III)}/\mathrm{Au}} - E^{o',\mathrm{H_2O}}_{\mathrm{DA^{2+}}/\mathrm{DA}} - \frac{RT}{6F}\ln\left(\frac{\left[\mathrm{Cl^-}\right]^{(4-\gamma)}\left[\mathrm{Fc^+}\right]^3}{\left[\mathrm{AuCl_{(4-\gamma)}(OH)_\gamma^-}\right]\left[\mathrm{Fc}\right]^3}\right) - \frac{RT}{F}\ln\left[\mathrm{H^+}\right]$$

Again, neglecting the 3rd term on the right-hand side for simplicity, one arrives at,

$$E_{cell} \approx E^{o',H_2O}_{Au(III)/Au} - E^{o',H_2O}_{DA^{2+}/DA} - \frac{RT}{F}\ln\left[H^+\right] \approx E^{o',H_2O}_{Au(III)/Au} - E^{o',H_2O}_{DA^{2+}/DA} + (0.0257\ V)(\ln 10)\left[H^+\right] \qquad [S5]$$

6. X-ray photoelectron, Fourier transform infrared, and UV/Vis spectroscopy data

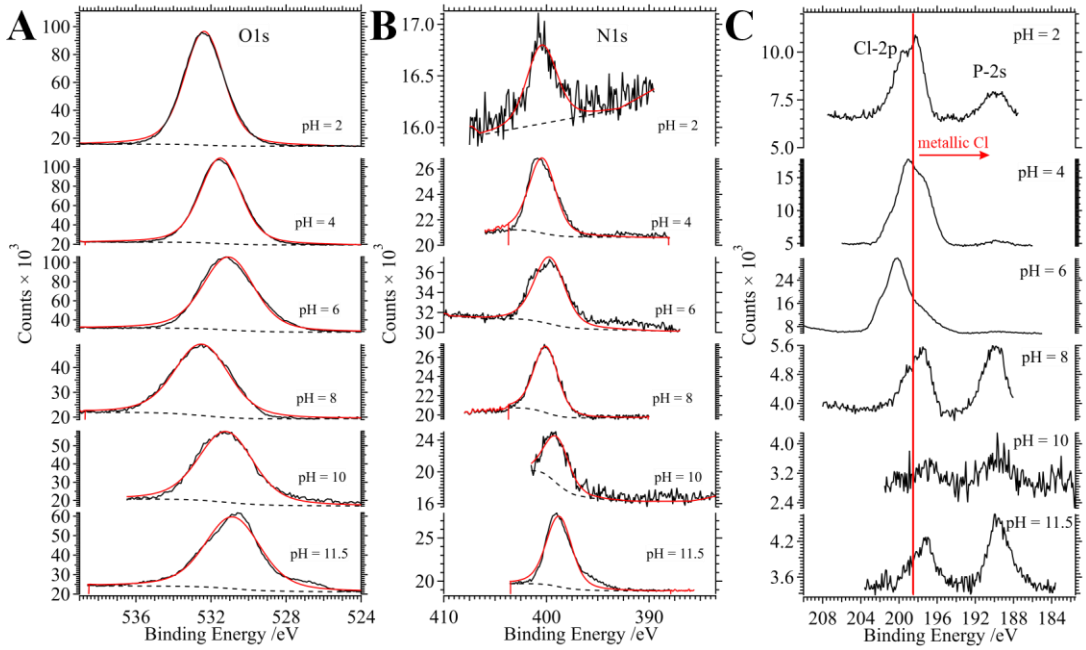

Figure S6: High-resolution XPS spectra recorded against films electrogenerated using Cell 1 at the aqueous pH indicated inset for the O 1s (**A**), N 1s (**B**), and Cl 2p (**C**) domains. Within C, a peak for P 2s is also visible.

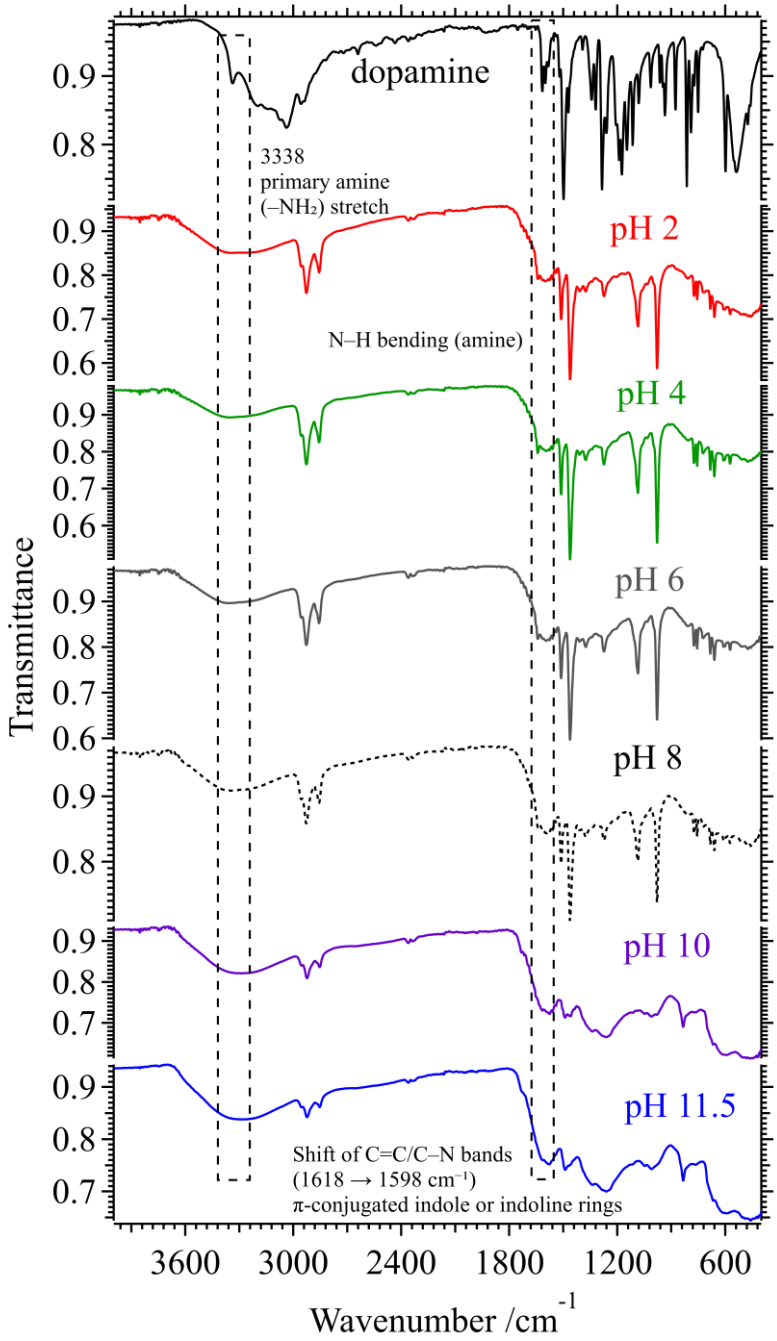

Figure S7: Fourier-transform infrared (FTIR) spectra recorded using dopamine or the Au NP/PDA film electrogenerated at the pH indicated inset.

7. References

1. M. Luty-Błocho, K. Pacławski, M. Wojnicki and K. Fitzner, *Inorg. Chim. Acta*, 2013, **395**, 189-196.
2. D. A. Skoog, *Principles of instrumental analysis*, Fourth edition. Fort Worth : Saunders College Pub., [1992] ©1992, 1992.

3. C. Johans, R. Lahtinen, K. Kontturi and D. J. Schiffrin, *J. Electroanal. Chem.*, 2000, **488**, 99-109.